RESEARCH ARTICLE | MARCH 11 2024

Modeling and algorithm for calculation the mixing and propagation of co-current flows in channels

Safar Khodjiev

AIP Conf. Proc. 3004, 060013 (2024)
https://doi.org/10.1063/5.0199839

Modeling and Algorithm for Calculation the Mixing and Propagation of Co-current Flows in Channels

Safar Khodjiev

Bukhara state university, 11, M.Ikbol str. Bukhara 200114, Uzbekistan

safar1951@yandex.ru

Abstract. This paper describes in detail the method and algorithm for calculating the numerical integration of non-stationary two-dimensional systems of Navier-Stokes equations for a compressible gas using high-order implicit (explicit) difference schemes, i.e. , the Beam- Warming difference scheme. A number of mathematical transformations , such as non-dimensionalization of coordinates and physical parameters, transforming the shape of the channel into a square one, as well as thickening the integration steps with large gradients of unknowns, which make it possible to bring problems to a model one for solving similar problems. In addition to the study, as convergence in the number of calculated points, the dependence of the number of iterations on the Courant number and comparison of the results obtained by different proposed models for calculating the effective viscosity, as well as a number of numerical studies as co- occurrence , temperature inhomogeneities, non- design , the ratio of the sizes of the inlet slots of cocurrent flows and the length of the channel to the height of the main flow and the degree of expansion of the channel to the process of mixing and distribution of flows in the channel. It was revealed at what ratios of the initial parameters of the cocurrent flows and the linear dimensions of the channel a recirculation zone is formed. For a channel of constant cross section at large ratios of velocities (72, 46) and temperature (2, 33), as well as small ratios of the channel length to the height of the inlet slot of the main flow (5, 31), even at the same jet pressures in the initial section, the recirculation zone occupies more than 55% of the input section, and the length along the longitudinal coordinate reaches 20 cm.

INTRODUCTION

Cocurrent gas jets is of exceptional importance in connection with the wide application of this process in the creation of rocket and space technology, gas lasers, mixing and combustion devices, combustion chambers of various power plants and in solving theoretical problems of turbulent exchange [1–7].

Theoretical and experimental studies of the existence conditions and sizes of recirculation zones during mixing of two flows of constant density are contained in [5, 6]. In [17, 6], the experimental results of the study are presented, and some features of the interaction of a supersonic jet with a limited co-flow are quantitatively determined. However, experimental studies and generalizations were mainly concerned with cases of a large ratio of the cross-sectional areas of flows at the channel inlet, when the active flow (jet, flow with high speed) was an axisymmetric jet in a channel of a significantly larger diameter [5, 6, 17].

The paper [16] describes the results of an experimental study and an attempt to generalize the geometric dimensions of the recirculation zones and the distribution of concentrations along the axis, with the flow of coaxial co-axial flows in a channel of constant cross section, and the cross-sectional areas of the flows at the inlet are comparable, and the passive flow is located along the axis of the channel.

It is relevant to solve such a problem by describing the mathematical model of internal laminar and turbulent flows, as well as its effective method of numerical solution.

As is known, at present, to describe the internal flow of a viscous gas, the complete system of Navier-Stokes equations [8–14] is used, the application of which opens up wide possibilities for a detailed description of a wide variety of flows. However, the numerical integration of this system is an extremely complex and time-consuming task, the solution of which is at the limit of the technical capabilities of existing computer technologies even in the case of a homogeneous viscous gas flow and requires efficient calculation methods and algorithms. [8,9,11,15,23 - 25].

This paper proposes a method and an efficient algorithm for the numerical study of the flow, displacement and propagation of cocurrent flows in channels of constant and variable cross sections.

PROBLEM STATEMENT

Let us consider the mixing and propagation of two viscous compressible gas flows in a channel of constant and variable cross-section of limited length $L$and half-height f_0. At the channel inlet, there are two streams with a longitudinal velocity u_1, temperature T_1, and pressure P_1, transverse jet height $f_0 - R_2$(wall jet), and a second longitudinal velocity u_2, temperature T_2, and pressure P_2, transverse jet height R_2, as well as data characterizing the physical properties of gas flows.

International Scientific and Practical Conference on "Modern Problems of Applied Mathematics and Information Technology (MPAMIT2022)"
AIP Conf. Proc. 3004, 060013-1–060013-11; https://doi.org/10.1063/5.0199839
Published by AIP Publishing. 978-0-7354-4876-6/$30.00

In mathematical modeling of the problem, we assume that the flow is viscous and two-dimensional, flat, and there are no body forces and heat supply from the outside. Taking into account the above assumptions and in the future, for the convenience of numerical solutions, by carrying out a series of mathematical transformations, such as selecting the appropriate scales for spatial coordinates and physical parameters, in the considered area leading to square and introducing condensing functions, which allow to condense the calculated points near the wall and the inlet part of the channel of the physical plane , while maintaining a constant step in the computational plane (in these areas, the flow is characterized by large gradients of gas-dynamic parameters), the above, taking into account the mathematical model of the problem under study, can be written in a vector-conservative form [8,9].

$$\frac{\partial U}{\partial t}+\frac{\partial F(U)}{\partial x}+\frac{\partial G(U)}{\partial y}=\frac{\partial V_1(U,U_x)}{\partial x}+\frac{\partial V_2(U,U_y)}{\partial x}+\frac{\partial W_1(U,U_x)}{\partial y}+\frac{\partial W_2(U,U_y)}{\partial y} \tag{1}$$

Relationship of total specific energy with internal and kinetic energy:

$$E=\rho\, C_\vartheta T+\frac{1}{2}\rho(u^2+\vartheta^2) \tag{2}$$

State equation:

$$p=\rho\, T \tag{3}$$

Expression for dynamic viscosity:

$$\mu=\mu_x+\mu_y \tag{4}$$

where μ_l- laminar, μ_t- turbulent viscosity, U- vector of conservative variables; F, G, V_1, V_2, W_1, W_2-flow vectors that look like:

$$U=\begin{bmatrix}\varphi_x & F_y & f & \rho & \\ \varphi_x & F_y & f & \rho & u \\ \varphi_x & F_y & f & \rho & \vartheta \\ \varphi_x & F_y & f & E & \end{bmatrix}=\begin{bmatrix}\bar{\rho}\\ \bar{\rho}u\\ \bar{\rho}\vartheta\\ \bar{E}\end{bmatrix}=\begin{bmatrix}\rho\\ m\\ n\\ E\end{bmatrix};\quad F=\frac{1}{L\varphi_x}\begin{bmatrix}m\\ \frac{m^2}{\rho}+p\\ \frac{mn}{\rho}\\ \frac{m(E+p)}{\rho}\end{bmatrix};\quad G=\frac{1}{F_y f}\begin{bmatrix}\Omega_1\rho\\ \Omega_1 m+\Omega P\\ \Omega_1 n+P\\ \Omega_1(E+P)\end{bmatrix}.$$

where $\Omega_1=(n+m\Omega)/\rho$, $\Omega=-\frac{yf'}{f}$.

$$V_1(U,U_x)=\frac{F_y f}{ReL^2\varphi_x}\begin{bmatrix}0\\ \frac{4}{3}\mu_x\\ N_x\\ \frac{nN_x}{\rho}+\frac{4}{3}\frac{mM_x}{\rho}+P_T T_x\end{bmatrix},\quad V_2(U,U_y)=\frac{1}{ReL}\begin{bmatrix}0\\ -\frac{2}{3}N_y+\frac{4}{3}\Omega M_y\\ M_y+\Omega N_y\\ \left(n+\frac{4}{3}\Omega m\right)\frac{M_y}{\rho}+\left(\Omega n-\frac{2}{3}m\right)\frac{N_y}{\rho}+\Omega P_T T_y\end{bmatrix},$$

$$W_1(U,U_x)=\frac{1}{ReL}\begin{bmatrix}0\\ N_x+\frac{4}{3}\Omega M_x\\ -\frac{2}{3}M_x+\Omega N_x\\ \frac{\left((m+\Omega n)N_x+\left(\frac{4}{3}\Omega m-\frac{2}{3}n\right)M_x\right)}{\rho}+\Omega P_T T_x\end{bmatrix},$$

$$W_2(U,U_y)=\frac{\varphi_x}{ReF_y f}\begin{bmatrix}0\\ [\frac{4}{3}\Omega^2+1]M_y+\frac{1}{3}\Omega N_y\\ (\Omega^2+\frac{4}{3})N_y+\frac{1}{3}\Omega M_y\\ \frac{\left(\left(\Omega^2+\frac{4}{3}\right)n+\frac{1}{3}\Omega m\right)N_y+\left(\left(\frac{4}{3}\Omega^2+1\right)m+n\right)M_y}{\rho}+(\Omega^2+1)P_T T_y\end{bmatrix},$$

Where $M_x = \frac{\hat{\mu}(m_x\rho - \rho_x m)}{\rho^2}, M_y = \frac{\hat{\mu}(m_y\rho - \rho_y m)}{\rho^2}, N_x = \frac{\hat{\mu}(n_x\rho - \rho_x n)}{\rho^2}, N_y = \frac{\hat{\mu}(n_y\rho - \rho_y n)}{\rho^2}, \ P_T = \frac{C_p\hat{\mu}}{Pr_T}$.
Here $f(x)$, the dimensionless shape of the channel, $L$is the dimensionless length of the channel, $\varphi(x)$and $F(y)$are, respectively, the thickening functions in the inlet and near-wall parts of the channel, the rest of the designations are generally accepted.

BOUNDARY AND INITIAL CONDITIONS

When setting the boundary conditions, we will assume that the channel of constant and variable cross section is symmetrical. In this case, we can confine ourselves to considering the flow in the region between the symmetry axis and one of the channel walls. The axis OXcorresponds to the axis of symmetry, and the OY channel height axis, which is specified as $y = f(x), x = 0$the channel inlet section, and the $f(0) = f_0$ half height of the channel inlet section, f_w c channel shade. The reduced system of differential equations (1) and relations (2 - 4) can be implemented using the following initial and boundary conditions, taking into account the channel at the inlet coaxially located to the nozzle R_2- height (indices 1,2, - $w$respectively, the parameters of the near-wall, central and on the wall)

$t = t_0$:

$$x = 0: \begin{cases} u = u_2, \vartheta = 0, E = E_2, \hat{\mu} = \hat{\mu}_2, \rho = \rho_2, p = p_2, \quad where\ 0 \le y \le R_2, \\ u = u_1, \vartheta = 0, E = E_1, \hat{\mu} = \hat{\mu}_1, \rho = \rho_1, p = p_1, \quad where\ R_2 < y < f_0, \\ u = 0, \vartheta = 0, E = E_w, \hat{\mu} = \hat{\mu}_w, \rho = \rho_w, p = p_w, \quad where\ y = 1. \end{cases} \tag{5}$$

$$0 < x \le 1: \begin{cases} u = 0, \vartheta = 0, E = E_0, \hat{\mu} = \hat{\mu}_0, \rho = \rho_0, p = p_0, \quad where\ 0 < y < 1, \\ u = 0, \vartheta = 0, E = E_w, \hat{\mu} = \hat{\mu}_w, \rho = \rho_w, p = p_w, \quad where\ y = 1. \end{cases}$$

$t > t_0$:

$$x = 0: \begin{cases} u = u_2, \vartheta = 0, E = E_2, \hat{\mu} = \hat{\mu}_2, \rho = \rho_2, p = p_2, \quad where\ 0 \le y \le R_2, & (6) \\ u = u_1, \vartheta = 0, E = E_1, \hat{\mu} = \hat{\mu}_1, \rho = \rho_1, p = p_1, \quad where\ R_2 < y < f_0, & (7) \\ u = 0, \vartheta = 0, E = E_w, \hat{\mu} = \hat{\mu}_w, \rho = \rho_w, p = p_w, \quad where\ y = 1. & (8) \end{cases}$$

$$0 < x \le 1: \begin{cases} \left.\begin{matrix} u = 0, \vartheta = 0, E = \tilde{E}_w \\ \rho = \tilde{\rho}_w, \dfrac{\partial P}{\partial \vec{n}} = 0, \hat{\mu} = \tilde{\mu}_w, T = \tilde{T}_w, \end{matrix}\right\} where\ \ y = 1 & (9) \\ \left.\dfrac{\partial u}{\partial y} = \vartheta = \dfrac{\partial E}{\partial y} = 0, \right\} where\ y = 0. & (10) \end{cases}$$

$$x = 1: \left\{\frac{\partial u}{\partial x} = \frac{\partial \vartheta}{\partial x} = \frac{\partial E}{\partial x} = 0 \ \left(or\ \frac{\partial^2 u}{\partial x^2} = \frac{\partial^2 \vartheta}{\partial x^2} = \frac{\partial^2 E}{\partial x^2}\right), where\ 0 < y < 1. \right. \tag{11}$$

Here $\rho_1, E_1, \hat{\mu}_1\ and\ \rho_2, E_2, \hat{\mu}_2$,, respectively, are calculated for a given temperature $T_1, T_2$and pressure of the p_1, p_2jet and cocurrent. The values $\rho_w, E_w, \tilde{\rho}_w, \tilde{E}_w, \tilde{\mu}_w$are calculated by setting the boundary conditions on the wall according to $u, \vartheta, T, P,\ and\ u_0, E_0, \rho_0, \mu_0, T_0$ are some initial values of the required parameters.

In all variants, the condition on the wall was set Pin the form

$$\left.\frac{\partial P}{\partial \vec{n}}\right|_w = 0 \tag{12}$$

It may seem that the condition is based on the boundary layer approximation, where $\frac{\partial \mathrm{P}}{\partial \mathrm{y}} \approx 0$ [10,19] is accepted. In reality, this condition is much less stringent, since constancy $P$is assumed not across the entire boundary layer, but only across the sublayer of thickness adjacent to the wall Δy. This method makes it possible to obtain a stable numerical solution both for flow in a continuous boundary layer and for flow with flow separation caused by the interaction of a shock wave with the boundary layer [11]. In the case of internal flows, setting the boundary conditions is complex and far from the final solution of the problem [12].

TRANSITION TO DIFFERENCE EQUATIONS AND CALCULATION METHOD

To integrate the vector equation (1) and relation (2 ÷ 4), we use the universal finite difference formula [9].

$$\Delta U^n = \frac{\theta\Delta t}{1+\theta_2}\frac{\partial}{\partial t}\Delta U^n + \frac{\Delta t}{1+\theta_2}\frac{\partial}{\partial t}U_n + \frac{\theta_2}{1+\theta_2}\Delta U^{n-1} \quad + O\left[\left(\theta - \frac{1}{2} - \theta_2\right)\Delta t^2 + \Delta t^3\right], \quad (13)$$

Where $\Delta U^n = U^{n+1} - U^n$.

This difference formula of a general form, due to the choice of parameters, θ *and* $\theta_2$makes it possible to obtain many conventional difference schemes [8, 9]. For schemes of the second order of accuracy $\bar{\theta}$, it is necessary to take equal to θ.

In practice, the scheme is implemented as follows [9]:

Step 1

$$\left[[I] + \frac{\theta\Delta t}{1+\theta_2}\left[\frac{\partial}{\partial x}([A] - [P] + [R_x])^n - \frac{\partial^2}{\partial x^2}([R])^n\right]\right]\Delta U^*$$
$$= \frac{\Delta t}{1+\theta_2}\left[\frac{\partial}{\partial x}(-\bar{F} + V_1 + V_2)^n + \frac{\partial}{\partial y}(-G + W_1 + W_2)^n\right] + \frac{\bar{\theta}\Delta t}{1+\theta_2}\cdot\left[\frac{\partial}{\partial x}(\Delta V_2)^{n-1} + \frac{\partial}{\partial y}(\Delta W_1)^{n-1}\right]$$
$$+ \frac{\theta_2}{1+\theta_2}\Delta U^{n-1} + O\left[\left(\theta - \frac{1}{2} - \theta_2\right)\Delta t^2, (\bar{\theta} - \theta)\Delta t^2, \Delta t^3\right] \quad (14)$$

Step 2

$$\left[[I] + \frac{\theta\Delta t}{1+\theta_2}\left[\frac{\partial}{\partial y}([B] - [Q] + [S_y])^n - \frac{\partial^2}{\partial y^2}([S])^n\right]\right]\Delta U^n = \Delta U^*; \quad (15)$$

Step 3

$$U^{n+1} = U^n + \Delta U^n \quad (16)$$

where $[A]^n = \left(\frac{\partial F}{\partial U}\right)^n$, $[B]^n = \left(\frac{\partial G}{\partial U}\right)^n, [R]^n = \left(\frac{\partial V_1}{\partial U_x}\right)^n$, $[R_x]^n = \left(\frac{\partial R}{\partial x}\right), [P]^n = \left(\frac{\partial V_1}{\partial U}\right)^n, [S]^n = \left(\frac{\partial W_2}{\partial U_y}\right)^n$, $[S_y]^n = \left(\frac{\partial S}{\partial y}\right)^n - J$ acobians. $I -$ a unit matrix of size 4×4.

We assume that at the beginning of the calculations ($t = n\Delta\, t_0$), at each node of the computational grid, all parameters of the initial flow are known from condition (5). The scheme given by equations (14) and (15) is three-layer and requires initial data on two layers. If they are absent, then the initial data on the second time layer can be obtained using a two-layer scheme, taking $\bar{\theta} = \theta_2 = 0$. For numerical integration of equations (14) and (15), the spatial derivatives are approximated to the second order $O(\Delta x^2;\ \Delta y^2)$.

The use of three-point approximation by central differences of the second order of accuracy for equations (14) (step 1.) and (15) (step 2.) leads to a finite-difference system of equations that have a block-tridiagonal structure.

The finite-difference system of equations for step 1 has the following form:

$$\begin{cases} \bar{A}_{1,j}\Delta U^*_{1,j} = \bar{D}_{1,j}, & i = 1, j = \overline{2, ny-1} \\ \bar{A}_{i,j}\Delta U^*_{i-1,j} + \bar{B}_{i,j}\Delta U^*_{i,j} + \bar{C}_{i,j}\Delta U^*_{i+1,j} = \bar{D}_{i,j}, & i = \overline{2, nx-1}, j = \overline{2, ny-1} \\ \bar{B}_{nx,j}\Delta U^*_{nx-1,j} + \bar{A}_{nx,j}\Delta U^*_{nx,j} = \bar{D}_{nx,j}, & i = nx, j = \overline{2, ny-1} \end{cases} \quad (17)$$

where nx *and* $ny$is the number of design points along the axes OX *and* OY, respectively, and $\bar{A}_{1,j}$, $\bar{D}_{1,j}$, $\bar{B}_{nx,j}$, $\bar{A}_{nx,j}$ *and* $\bar{D}_{nx,j}$, are vectors (actually a square matrix with size 4×4, where only the elements of the first diagonal can be non-zero) and they can be 0 or 1, $\bar{A}_{i,j}, \bar{B}_{i,j}, \bar{C}_{i,j}, \bar{D}_{i,j}$ are known coefficients calculated from the previous iteration.

Using matrix sweep, [21,22] it is easy to obtain solution (17) in the recurrent form

$$\Delta U^*_{i,j} = \alpha_{i,j}\Delta U^*_{i+1,j} + \beta_{i,j}, \qquad i = \overline{nx-1, 2}, j = \overline{2, ny-1} \quad (18)$$

Where $\alpha_{i,j}, \beta_{i,j} -$ sweep coefficients, also calculated by recursive formulas

$$\alpha_{i,j} = -\left(\bar{A}_{i,j}\alpha_{i-1,j} + B_{i,j}\right)^{-1}\bar{C}_{i,j}, \qquad \beta_{i,j} = \left(\bar{A}_{i,j}\alpha_{i-1,j} + B_{i,j}\right)^{-1}\left(\bar{D}_{i,j} - \bar{A}_{i,j}\beta_{i-1,j}\right),$$
$$i = \overline{2, nx-1}, j = \overline{2, ny-1} \quad (19)$$

B (19)$\alpha_{1,j}$ *and* $\beta_{1,j}$ are determined from the boundary conditions at $i = 1$ from the first equation of system (17). Boundary conditions at $x = 0$ (5) *and* $x = L$ $(x = 1)$ (11) are implicitly implemented with respect to conservative variables. ρ, n, m, E. The equation

$$\bar{A}_{1,j}\Delta U^*_{1,j} = \bar{D}_{1,j} \quad (20)$$

corresponds to the rigid boundary condition at the channel input, for all $j = \overline{1, ny-1}$. The known values of the variables ρ, n, m, E at the input $(i = 1)$ make it possible to determine $\alpha_{1,j}$ and $\beta_{1,j}$ from equation (20) in the form:

$$\alpha_{1,j} = 0;\ \beta_{1,j} = \bar{A}_{1,j}^{-1}\bar{D}_{1,j};\quad j = \overline{1, ny-1} \tag{21}$$

It should be noted that the third equation (17), i.e.

$$\bar{B}_{nx,j}\Delta U_{nx-1,j}^{*} + \bar{A}_{nx,j}\Delta U_{nx,j}^{*} = \bar{D}_{nx,j}, \qquad j = \overline{2, ny-1} \tag{22}$$

corresponds to the boundary condition (11).

Using Eqs. (18) and (22) for $i = nx$, we find the solution $\Delta U_{nx,j}^{*}$,

$$\Delta U_{nx,j}^{*} = \left(\bar{B}_{nx,j}^{-1}\cdot\bar{A}_{nx,j} + \alpha_{nx-1,j}\right)^{-1}\left(\bar{B}_{nx,j}^{-1}\cdot\bar{D}_{nx,j} - \beta_{nx-1,j}\right),\ j = \overline{2, ny-1} \tag{23}$$

and then successively the rest of the value $\Delta U_{i,j}^{*}$ from (18). If instead of condition (11) an "output" condition of the form

$$\frac{\partial^2 u}{\partial x^2} = \frac{\partial^2 \vartheta}{\partial x^2} = \frac{\partial^2 E}{\partial x^2} = 0,$$

finite difference equation

$$\bar{A}_{nx,j}\Delta U_{nx-2,j}^{*} + \bar{B}_{nx,j}\Delta U_{nx-1,j}^{*} + \bar{C}_{nx,j}\Delta U_{nx,j}^{*} = \bar{D}_{nx,j}, \qquad j = \overline{2, ny-1} \tag{24}$$

in the joint solution of the following system of equations

$$\bar{A}_{nx-1,j}\Delta U_{nx-2,j}^{*} + \bar{B}_{nx-1,j}\Delta U_{nx-1,j}^{*} + \bar{C}_{nx-1,j}\Delta U_{nx,j}^{*} = \bar{D}_{nx-1,j}, \qquad j = \overline{2, ny-1}$$
$$\Delta U_{nx-1,j}^{*} = \alpha_{nx-1,j}\Delta U_{nx,j}^{*} + \beta_{nx-1,j} \tag{25}$$

calculated $\Delta U_{nx,j}^{*}$ by the formula

$$\Delta U_{nx,j}^{*} = \left[\left(\bar{A}_{nx,j}^{-1}\bar{B}_{nx,j} - \bar{A}_{nx-1,j}^{-1}\bar{B}_{nx-1,j}\right)\alpha_{nx-1,j} + \left(\bar{A}_{nx,j}^{-1}\bar{C}_{nx,j} - \bar{A}_{nx-1,j}^{-1}\bar{C}_{nx-1,j}\right)\right]^{-1}\times$$
$$\times\left[\bar{A}_{nx,j}^{-1}\bar{D}_{nx,j} - \bar{A}_{nx-1,j}^{-1}\bar{D}_{nx-1,j} - \left(\bar{A}_{nx,j}^{-1}\bar{B}_{nx,j} - \bar{A}_{nx-1,j}^{-1}\bar{B}_{nx-1,j}\right)\beta_{nx-1,j}\right] \tag{26}$$

After finding $\Delta U_{nx,j}^{*}$ the finite-difference system of equations (17) at all internal points, we proceed to the numerical integration of equations (15) (Step 2). We find solutions in the same way $\Delta U_{i,j}$. It should be noted that the use of various boundary conditions on the wall, for example, of the type $\left(\frac{\partial T}{\partial \vec{n}} = 0; \frac{\partial P}{\partial \vec{n}} = 0\right)$ or others, greatly complicates the implementation of the scheme proposed in [9]. Therefore, in Step 2 it is assumed that the solution for the desired variables within these boundaries is known from the (n)th time layer. It is safe to say that such an assumption does not affect the convergence in the least when steady solutions are found.

On the axis of symmetry for the boundary condition (10), an implicit implementation procedure is applied, then finding a solution $\Delta U_{i,j}^{n}$ same as described in step 1.

The implementation of the scheme for calculating steady-state solutions in time can be represented in the following sequence:

1. At the moment of time, the $t = t_0$ initial values of all the required variables are set;
2. Solutions are found $\Delta U_{i,j}^{*}$ and boundary conditions (9 ÷ 10) are satisfied;
3. Solutions are found $\Delta U_{i,j}^{n}$ and boundary conditions (11) are satisfied;
4. Solutions are found $\Delta U_{i,j}^{n+1}$ by formula (16), step 3;
5. From equality (2) is calculated $T_{i,j}^{n+1}$;
6. From the equation of state is determined $P_{i,j}^{n+1}$;
7. The effective turbulent viscosity is calculated $\hat{\mu}_{i,j}^{n+1}$ using the formula:

$$\hat{\mu} = const T^{0,6472} + \chi\rho b^2(x)\left|\frac{\partial u}{\partial y}\right|, \tag{27}$$

where χ is the empirical turbulence constant, is $b(x)$ the conditional width of the mixing area;

8. Convergence (establishment) of the solution by the condition is checked

$$\max_{i,j}\left|\frac{\Delta U_{i,j}^{n}}{U_{i,j}^{n}\Delta t}\right| < \varepsilon \tag{28}$$

where ε is a small number.

If conditions (28) are not satisfied, then the calculation process is repeated from the second point, otherwise it is considered that the steady-state solution with accuracy ε found.

IMPLEMENTATION OF THE METHOD AND RESULTS OF METHODOLOGICAL CALCULATIONS

The described method and algorithm were implemented as a program. This program can be used to calculate laminar and turbulent flows in flat channels of constant and variable (in Laval nozzles) sections, as well as jet flows for a limited co-current flow.

It should be noted that all variants of the boundary conditions for temperature (of the first and second kind), velocity (sticking, sliding) on the wall and at the outlet, specific design points along the axes x *and* y, as well as the thickening coefficients K_x *and* K_y[13] and setting the shape (dimensions) of the channel are included in the set of initial data, therefore, when solving a wide range of specific problems, it is not necessary to make any changes to the text, and in this sense the program is universal.

For carrying out methodical calculations, a flat channel was chosen as an object, for which the ratio of length to half-height was 5, and the Reynolds number $Re$was calculated from the initial values of density, velocity, half-height of the channel and dynamic viscosity, its given power dependence on T[14].

As initial conditions $(t = t_0)$, i.e., the longitudinal velocity component, pressure and temperature were considered constant, and the transverse velocity component was assumed to be zero everywhere. Dynamic viscosity at each design point was calculated by the formula

$$\mu_e = const T^{0,6472} \tag{29}$$

and thermal conductivity according to the formula $\lambda = \frac{C_P \hat{\mu}}{Pr}$,

where $const$in (29) is calculated by the method given in [14].

The dimensionless time step in each iteration is chosen from the condition [15] $\Delta t \le min\left(\Delta t_x, \Delta t_y\right)$, where

$$\Delta t_x \le \frac{1}{2}\frac{1}{\frac{|u|+\bar{a}}{L\Delta x \varphi_x} + \frac{2\gamma}{Re\rho L^2 \varphi_x^2 \Delta x^2}}, \Delta t_y \le \frac{1}{2}\frac{1}{\frac{|\vartheta|+\bar{a}}{F_y \Delta y} + \frac{2\gamma}{Re\rho F_y^2 \Delta y^2}}, \gamma = max\left[\hat{\mu}, \frac{4}{3}\hat{\mu}, \lambda\right] \tag{30}$$

Here $\bar{a}$ is the speed of sound.

The fulfillment of condition (28) was considered as the criterion for establishing accuracy in methodological calculations, and at the same time ε= 0.0001 ÷ 0.0005 was taken in the calculations.

Of great interest is the choice of a mathematical model for calculating the effective viscosity [8,19]. For this purpose, we study a jet flowing out of a flat slot and propagating in a cocurrent air flow in a flat channel of constant cross section. As the basic object of study, a channel was chosen, similarly to [17], with geometric characteristics $D = 188\,mm$ ($f_0 = 94\,mm, L = 1{,}4\,m$).

In the calculations it was taken: $T_1 = T_2 = 300\,K, P_1 = P_2 = P_{atm} = 1\,atm, \mathrm{Pr}_T = 0{,}7$. Options for calculating the effective turbulence using formulas (27) were considered, and

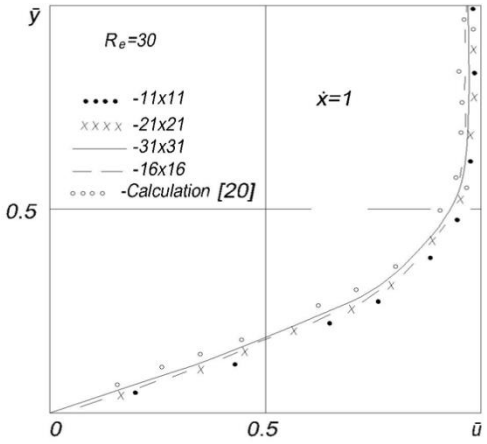

Figure 1. Velocity profiles on the channel slice with a different number of calculated points in the transverse and longitudinal directions.

$$\hat{\mu}_T = \chi b(x)(\rho u)|_{y=0} \tag{31}$$

$$\hat{\mu}_T = \chi b^2(x)\rho\frac{\partial u}{\partial y}. \tag{32}$$

Numerical calculations have shown that formulas (27) and (32) give practically the same results for subsonic displacements. For the displacement of supersonic flows, $\left(\frac{u_2}{u_1} = 1{,}4706,\ \frac{R_2}{f} = 0{,}26\right)$ the results in the near-wall region and in the region of flow contact are noticeably different (Figure 1).

This can be explained by the fact that when two viscous flows with different velocities are displaced, the drag coefficient increases at the displacement boundary. Of these algebraic models, formula (27) was used to calculate the effective turbulent viscosity in serial calculations.

To study the convergence of the scheme and the reliability of the numerical results, series of air flow calculations were carried out on a grid with different steps and for the same air parameters based on the narrow channel approximation model [20]. Obtaining convergence in different grids and qualitative coincidence of the

results with the work [20] indicates the reliability of the results and the correctness of the calculation algorithm (Figure 2).

With the help of the above method and the calculation program, a number of studies have been carried out, such as non- isothermality , satellite and the ratio of satellite height , off - design $\left(\frac{P_2}{P_1} \neq 1\right)$, channel length and under different boundary conditions on the wall, as well as the degree of channel expansion due to displacement and flow propagation in a flat channel.

Figure 3 shows the transverse temperature distribution in different sections along the longitudinal coordinate at the same temperatures$\left(\frac{T_2}{T_1} = 1\right)$ cocurrent options:

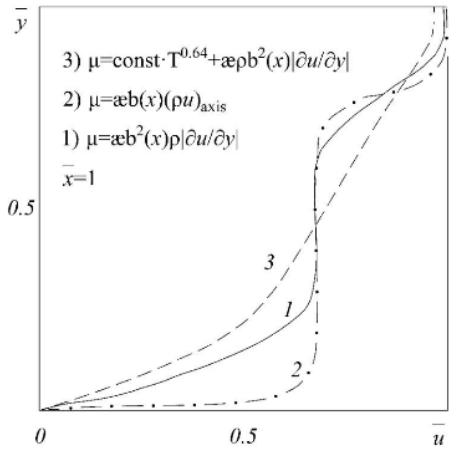

Figure 2. Velocity profiles on the channel slice for different models of the turbulent viscosity coefficient.

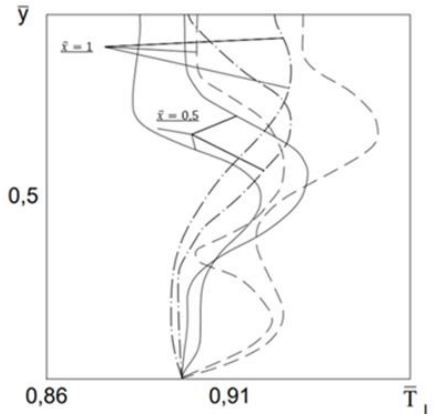

Figure 3. Temperature profiles at different distances from the inlet section of the channel:

– – – - $\frac{u_2}{u_1} = 0.0965; \frac{R_2}{f_0} = 0.5; \frac{h}{f_0} = 14.8936$

_____ - $\frac{u_2}{u_1} = 45.0725; \frac{R_2}{f_0} = 0.5; \frac{h}{f_0} = 14.8636$

–.–.– - $\frac{u_2}{u_1} = 10.367; \frac{R_2}{f_0} = 0.26; \frac{h}{f_0} = 14.8636$

№ 1. $\frac{u_2}{u_1} = 0{,}0965, \frac{R_2}{f_0} = 0{,}5, \frac{L}{f_0} = 14{,}8936$

№ 2. $\frac{u_2}{u_1} = 45{,}0725, \frac{R_2}{f_0} = 0{,}5, \frac{L}{f_0} = 14{,}8936$

№ 3. $\frac{u_2}{u_1} = 10{,}3667, \frac{R_2}{f_0} = 0{,}26, \frac{L}{f_0} = 14{,}8936$

As can be seen from these results, the temperature increases in the mixing regions, and in the initial part of the channel it is lower than in the outlet. $(\hat{x} = 1)$. This is explained by the fact that at the mixing boundary, due to the deceleration of the flow, the gradient of velocity and friction increases, and this, in turn, leads to an increase in temperature. In the variant № 2, a recirculation zone is observed in the initial section of the channel and reaches 25% of the inlet half-height of the inlet section.

Studies of the influence of non- isothermality in the range $0{,}6 < \frac{T_2}{T_1} < 2{,}3333$at constant pressure of the jet and co-flow are mutually equal and at $\frac{T_2}{T_1} = 2{,}3333, \frac{u_2}{u_1} = 0{,}0222$values $\frac{R_2}{f_0} = 0{,}26$and 0.5 in the mixing region, no sharp changes in the velocity and temperature profiles are observed, and in both cases the core and high temperature are maintained until the end of the channel. At $\frac{T_2}{T_1} = 0{,}4286, \frac{u_2}{u_1} = 0{,}0222$ $\left(\frac{R_2}{f} = 0{,}5, \frac{L}{f} =\right.$

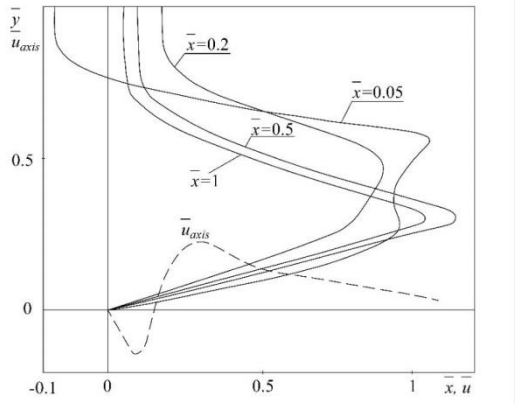

Figure 4. Transverse profiles of the longitudinal velocity in different section of the channel and its axial changes along the channel at

$-\frac{u_2}{u_1} = 0.0222; \frac{R_2}{f_0} = 0.5; \frac{h}{f_0} = 5.3191; \frac{T_2}{T_1} = 2.3333; \frac{P_2}{P_1} = 1.$

$5{,}3191\big)$, i.e., the temperature and flow velocity that is supplied to the central part of the channel is much less than in the near-wall part, so that with such an option for studying the mixing and distribution of two viscous air flows near the mouth of the channel, a recirculation zone is formed (Figure 4), and when moving away from the inlet part of the channel, the recirculation zone is not observed.

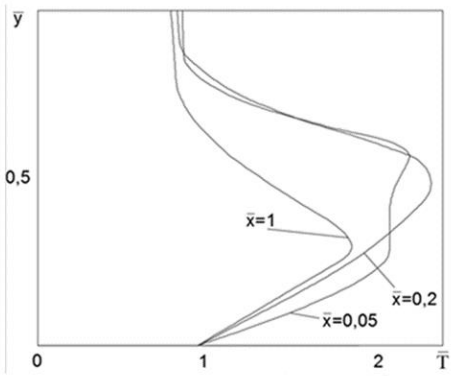

Figure 5. Temperature profiles at different distances from the inlet section of the channel at $-\frac{u_2}{u_1} = 0{,}0222$; $\frac{R_2}{f_0} = 0{,}5$; $\frac{h}{f_0} = 5{,}3191$; $\frac{T_2}{T_1} = 2{,}3333$; $\frac{P_2}{P_1} = 1$

In the mixing regions, in the initial section of the channel, the deceleration of the peripheral flow velocity at the mixing boundary is observed, while the transverse distribution of the longitudinal velocity has a saddle shape, and with distance the maximum velocity value shifts to the channel axis and takes on a parabolic form. The opposite behavior is observed in the transverse temperature distribution along the channel, i.e., near the mouth of the channel at the mixing boundary of two flows, friction increases due to viscosity, and this, in turn, leads to an increase in the flow temperature (Figure 5).

It was found that at large ratios of velocities $\left(\frac{u_2}{u_1} = 72{,}4636\right)$, as well as small ones $L/f = 5{,}3191$ ($T_2/T_1 = 2{,}3333, R_2/f = 0{,}26$in the initial section, the recirculation zone occupies about 55–60 % of the inlet section, and the length along the longitudinal coordinate reaches 20 cm, which is confirmed by the experimental materials of works [16,17].

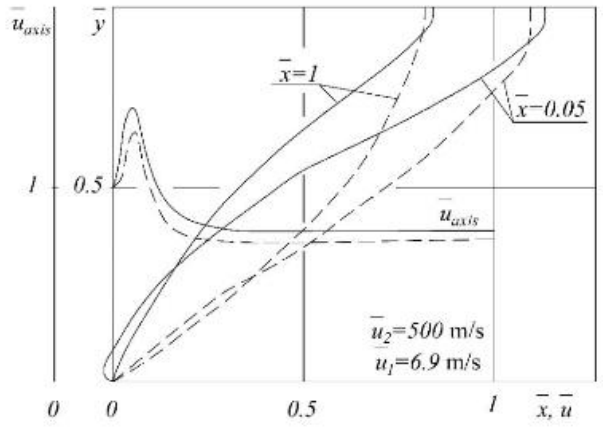

Figure 6. Transverse distribution of the longitudinal velocity at different distances from the inlet section of the channel, and its axial change along the channel:
___ - $\frac{u_2}{u_1} = 72{,}4636; \frac{R_2}{f_0} = 0.5; \frac{h}{f_0} = 14.8936; \frac{T_2}{T_1} = 1; \frac{P_2}{P_1} = 2.$
− − −- $\frac{u_2}{u_1} = 72{,}4636; \frac{R_2}{f_0} = 0.5; \frac{h}{f_0} = 14.8936; \frac{T_2}{T_1} = 2.333; \frac{P_2}{P_1} = 2.$

In this variant, in the initial section of the channel, in the area where the flows come into contact, the longitudinal velocity noticeably increases. This can be explained by the fact that the jet is supersonic, and the velocity of the cocurrent flow is rather low $u_1 = 6{,}9$m/s, and naturally, the jet behaves as if it is flowing into an expanding area with distance from the inlet, the velocity and temperature on the axis decrease.

Of great practical interest is the study of the influence of initial pressures, temperatures, the co-occurrence parameter of mixing flows and the geometric ratio of the sizes of the slots in the channel on the features of mixing and propagation of the air flow.

Here are some numerical results related to non- calculation cocurrent flows under identical $\frac{u_2}{u_1} = 72{,}4638, \frac{R_2}{f_0} = 0{,}5, \frac{L}{f_0} = 14{,}8936$and conditions on the wall $\frac{\partial \mathrm{T}}{\partial \mathrm{y}} = 0$.

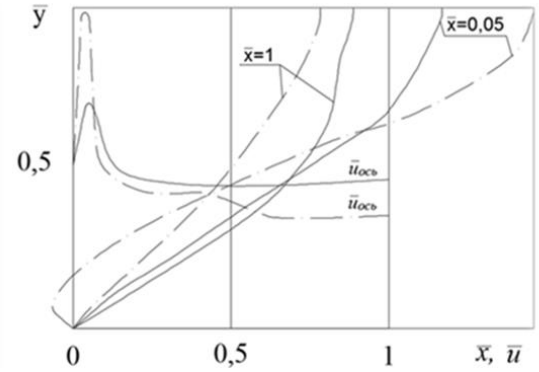

Figure 7. Transverse distribution of the longitudinal velocity at different distances from the nozzle cutoff, as well as its axial change along the channel: −Opt.№20, Opt.№21
___ - $\frac{u_2}{u_1} = 72{,}4636; \frac{R_2}{f_0} = 0.5; \frac{h}{f_0} = 14.8936; \frac{T_2}{T_1} = 1; \frac{P_2}{P_1} = 4.$
− − − - $\frac{u_2}{u_1} = 72{,}4636; \frac{R_2}{f_0} = 0.5; \frac{h}{f_0} = 14.8936; \frac{T_2}{T_1} = 2.333; \frac{P_2}{P_1} = 4.$

In Figure 6. the transverse distribution of the longitudinal velocity is given at various distances from the channel exit at the same jet and coflow temperatures , i.e. $T_1 = T_2 = 300\ K$, as well as at $T_1 = 300\ K\ and\ T_2 = 700\ K, and\ \frac{p_2}{p_1} = 2$. As follows from the graph, with an increase in the jet temperature, $T_2 = 700\ K$reverse currents are traced, i.e., recirculation zones in the initial sections. At the same temperatures of the jet and cocurrent, this is not observed. Increasing the temperature of the jet promotes the development of the flow. The axial value of the longitudinal velocity is also given here. As can be seen from the graph, the axial value of the velocity first increases, and decreases with distance from the channel cutoff. This is explained by the fact that an increase in temperature leads to an acceleration of the flow and a decrease in pressure in the initial sections. Figure 7 shows the transverse distribution of the longitudinal velocity on different longitudinal sections of the channel at the same temperatures of the jet and cocurrent flow ($T_1 = T_2 = 300\ K$)and at the jet temperature $700\ K$, and the cocurrent flow $-300\ K$, as well as the jet pressure of 4 atm and the cocurrent flow of 1 atm. As follows from the results, an increase in the temperature and pressure of the jet leads to an increase in the recirculation zone of the flow in the initial sections of the channel and the rapid development of the flow. From the given axial values of the longitudinal velocity, it can be noted that an increase in the initial values of the temperature and pressure of the jet leads to a sharp increase in the axial values of the longitudinal velocity in the initial sections of the channel, and when moving away from the channel exit, to its rapid drop. Such patterns were observed in [16, 17].
The obtained numerical results make it possible to regulate the flow in the channels for specific ratios of the parameters of the cocurrent flows and the geometry of the channel.

CONCLUSION

On the basis of the conducted method and algorithm for calculating numerical solutions of the Navier – Stokes equations for the flow of compressible gas, the effects of entanglement, non-isothermicity, the ratio of the height of the slots, the uncountability of co-flows and the length of the channel on the parameters of mixing and propagation of co-flows in the channel are investigated, and it is also revealed at what ratios of these parameters the recirculation zone is observed. It is revealed that the effects of non-isothermicity in the range $0{,}6 < T_2/T_1 < 2{,}333$ at the same pressure of the jet and co-flows in the mixing region, sharp changes in the velocity and temperature profiles are not observed, and the core and high temperature remain until the end of the channel. It is revealed that at

high velocity ratios (u_2/u_1=72.4636), as well as small values L/f_0= 5.319 and R_2/f_0=0.26 (T_2/T_1=2.333) in the initial section of the channel, the recirculation zone occupies about 55-60% of the input section, and the length along the longitudinal coordinate reaches 20 cm, as well as an increase in temperature and the pressure of the jet leads to an increase in the recirculation zone of the flow in the initial sections and the rapid development of the flow.

REFERENCES

1. G. N. Abramovich, S. Yu. Krashennikov, A. N. Sekundov, and I. N. Smirnov, *Turbulent mixing of gas jets* (Moscow Nauka 1974).
2. Yu.V.Vinogradov, V.N.Gruzdev, V.F.Postnov and A.V.Talantov, "Characteristics of turbulence during the flow of co-current flat jets in a closed channel" (Izv.AN USSR. MJG, 1977) No 2 pp. 175-178.
3. K.S.Dzhaugashtin and A.L.Yarin, "Aerodynamics of a coaxial jet" V.Kn .: Theory and practice of gas combustion. VII.- L: Nedra, pp.11-15 (1981).
4. V. F. Postnov, V. N. Gruzdev, and et al., "Propagation of a flat isothermal jet in a cocurrent limited flow" Aviation technology, No. 1, pp. 71-77 (1976).
5. A.Graya and R.Curtet, "Riblications Scientifigues et technologues du ministere de L'Air" , Mars, no. 359 (1960).
6. M.Barchilon, and R.Curtet, "Trans ASME", Ser. D.4. (1964).
7. Yu.V.Vinogradov, V.N.Gruzdev, and A.V.Talantov, "Influence of turbulence intensity on the processes of mixing of wake jets at different velocity ratios", In the book: Theory and practice of gas combustion. Issue. V. - L.: Nedra, pp. 28-33 (1972).
8. D.Anderson, J.Tannekhil, and R.Pletcher, "Computational fluid mechanics and heat transfer" In 2 T. T.2. per. from English. -M: Mir, pp. 392-728 (1990).
9. R. M. Beam and R. F. Warming, "Implicit factorized difference scheme for the Navier-Stokes equation for a compressible gas flow" Rocket technology and astronautics. Translation from English, Vol. 16, No. 4, S. 145-15 (1978).
10. G.Schlichting, *Theory of the boundary layer* (Moscow Nauka, 1974).
11. P.Roach, *Computational fluid dynamics* (Per. from English. Moscow Mir, 1980).
12. Yu.V.Lapin, O.A.Nekhamkina, V.A.Pospelov, M.Kh.Sagittarius, and M.L.Shur, "Numerical modeling of internal flows of viscous chemical reacting gas mixtures. Results of science and technology", Ser. Mechanics of liquid and gas. T.19.M., pp. 86-185 (1985).
13. S.Khodzhiev, Z.Sh.Zhumaev, and O.O.Yodgorov, "Numerical calculation of internal flows of a compressible gas using an implicitly factorized difference scheme", Izv. Academy of Sciences of the Uzbek SSR. STN. Tashkent, Fan. No. 2. pp.28-34 (1990).
14. Yu.V.Lapin, and M.Kh.Sagittarius, *Internal flows of gas mixtures,* (Moscow Science. Editor-in-Chief. Physics and Mathematics, 1989).
15. R.V.MacCormac, "Numerical method for solving the equations of viscous compressible flows", Aerospace engineering. T.11. No. 4, pp. 114-123 (1983).
16. V.K.Baev, V.A.Konstantinovsky, and I.V.Sidorov, "Mixing of cocurrent flows in a channel of constant cross section in the presence of a recirculation zone" Physics of combustion and explosion, No. 1, pp. 70-76 (1972).
17. L.A.Bakaldina, and I.V.Sidorov, "Conditions for the existence and longitudinal dimensions of recirculation zones during the interaction of a supersonic jet with a limited cocurrent subsonic flow", Izv.SO An USSR, No.8, issue 2, pp.37-45 (1970).
18. J.Boussinesq, and Essai Sur la "Theorie Des Eaux Courantes", Mem.Presentes Acad. Scl., v. 23, Paris. p.46 (1877).
19. L.G.Loitsyansky, *Mechanics of liquid and gas,* (Moscow Nauka, 1987).
20. M. P. Manina, V. A. Pospelov, and S. Khodjiev, "Solutions of the Direct Problem of the Laval Nozzle in the Narrow Channel Approximation by the Establishment Method," Zh.L. Collection of scientific works . LPI "Hydroaerodynamics", pp. 26-30 (1983).
21. R.Richtmaer, and K.Morton, *Difference methods for solving boundary value problems*. // Translation from the second English edition, edited by B.M. Budak and A.D. Gorbunov. (Moscow Mir, 1972).
22. A.A.Samarsky, *Theory of difference schemes,* (Moscow Nauka, 1977).
23. S. Khodjiev. "Modeling and calculation method of mixing and propagation of co-current flows in channels" Abstracts of the international scientific-practical conference "Modern problems of applied mathematics and information technology", Bukhara, May 11-12. 366 p.(2022).

24. Ye.V.Buryatskiy, A.G.Costini, and et.al., “Metod for numerical solution of the Navier-Stokes equations in velocity-pressure variables”, ISSN 1561. Applied g. i. dromechan i. ka. Volume 10, No. 2. pp. 13-28 (2008).
25. V.M. Kovenya, “On one algorithm for solving the Navier-Stokes equations for a viscous incompressible fluid” Computing technique. Novosibirsk. Volume 11, No. 2, pp. 39-51 (2006).